Available online at www.sciencedirect.com
SCIENCE DIRECT®
PHYSICS LETTERS A
ELSEVIER
Physics Letters A 314 (2003) 315–321
www.elsevier.com/locate/pla

Localized electron states near pentagons in variously shaped carbon nanoparticles

R. Pincak [1,*] V.A. Osipov

Joint Institute for Nuclear Research, Bogoliubov Laboratory of Theoretical Physics, 141980 Dubna, Moscow region, Russia

Received 24 April 2003; accepted 4 June 2003

Communicated by R. Wu

Abstract

The electronic structure of variously shaped carbon nanoparticles (nanocone, fullerene, and hyperboloid) is investigated within a gauge field-theory model. Both the eigenfunctions and the local density of states (DOS) near the pentagonal defects are numerically calculated. The numerical study shows that the low-energy DOS has a cusp which drops to zero at the Fermi energy for any number of pentagons at the tip except three. For three pentagons, the nonzero DOS across the Fermi level is formed. The peculiarities in the case of graphitic hyperboloid are discussed.

PACS: 73.20.Dx; 73.50.Jt; 73.61.Wp

1. Introduction

In experiment, there were produced variously shaped carbon nanoparticles: nanotubes, fullerenes, cones, toroids, graphitic onions, nanohorns, etc. It has been found that the electronic properties of these nanoparticles can be remarkably modified due to the presence of pentagons in the hexagonal carbon lattice. In particular, the localized electronic states near pentagons has been observed in some carbon nanoparticles by scanning tunneling microscopy (STM) [1,2]. Recently, the electronic structure of a single pentagon has been revealed on an atomic scale by STM [3] where the enhanced charge density at the pentagon has been experimentally clarified.

The peculiar electronic states near the pentagons in curved graphite nanoparticles were the subject of intensive theoretical studies in fullerenes [4,5], nanotubes [6], and cones [7,8]. In particular, an analysis within the effective-mass theory has shown that a specific $\sqrt{3} \times \sqrt{3}$ superstructure induced by pentagon defects can appear in nanocones [9]. This prediction has been experimentally verified in [3]. A recent study [10] within both tight-binding and ab initio calculations shows a presence of sharp resonant states in the region close to the Fermi energy. The strength and the position of these states with respect to the Fermi level was found to depend sensitively on the number and the relative positions of the pentagons constituting

* Corresponding author.
E-mail addresses: pincak@saske.sk (R. Pincak), osipov@thsun1.jinr.ru (V.A. Osipov).
[1] On leave from Institute of Experimental Physics, Slovak Academy of Sciences, Watsonova 47, 043 53 Kosice, Slovak Republic.

0375-9601/$ – see front matter
doi:10.1016/S0375-9601(03)00898-3

the conical tip. In particular, a prominent peak which appears just above the Fermi level was found for the nanocone with three symmetrical pentagons (which corresponds to a 60° opening angle or, equivalently, to 180° disclination). A similar result has been recently obtained in the framework of the gauge-theory approach [8]. Notice also that localized cap states in nanotubes has been recently studied in [11].

The aim of this Letter is to study numerically the problem of electron states in carbon nanostructures for three geometries: sphere, cone, and hyperboloid. The model equations in each case are constructed by using two basic theories: the effective-mass theory for a graphite monolayer [12] and the gauge theory of disclinations on fluctuating elastic surfaces [13]. Notice that pentagons in graphite lattice are the topological defects in their origin (disclinations). Finally, the model is formulated as the Dirac equation on a curved surface with a flux due to a pentagonal apical disclination represented by Abelian gauge field.

2. The model

The effective-mass theory for a two-dimensional graphite lattice is equivalent to the $\vec{k}\cdot\vec{p}$ expansion of the graphite energy bands about the $\vec{K}$ point in the Brillouin zone [12]. In fact, there are two kinds of sublattice points in a unit cell (two degenerate Bloch eigenstates at $\vec{K}$), so that the wave function can be approximated by

$$\Psi(\vec{k},\vec{r}) = f_1(\vec{\kappa})e^{i\vec{\kappa}\vec{r}}\Psi_1^S(\vec{K},\vec{r}) + f_2(\vec{\kappa})e^{i\vec{\kappa}\vec{r}}\Psi_2^S(\vec{K},\vec{r}),$$

where $\vec{k} = \vec{K} + \vec{\kappa}$. In the linear in $\vec{\kappa}$ approximation, the Schrödinger equation is reduced to the secular equation for functions $f_{1,2}(\vec{\kappa})$. After diagonalization, it finally results in the two-dimensional Dirac equation [12]

$$i\gamma^\mu\partial_\mu\psi(\vec{r}) = E\psi(\vec{r}), \tag{1}$$

where γ^μ are the conventional Pauli matrices: $\gamma^1 = -\sigma^2$, $\gamma^2 = \sigma^1$, the energy E is accounted from the Fermi energy, and the two-component wave function ψ represents two graphite sublattices. In our case, the model (1) must be generalized in two ways. First, one has to incorporate nontrivial geometry and, second, to include a disclination field in (1).

In accordance with the basic assumption of the gauge approach, disclinations can be incorporated by means of introducing dynamical $SO(2)$ gauge fields (compensating Yang–Mills fields) in the Lagrangian of elasticity theory [13]. It was found that the elastic flux due to rotational defects is completely determined by the gauge vector fields associated with disclinations. In this context, disclination field can be simply accounted in (1) by using the covariant derivative. Finally, the Dirac equation (1) on an arbitrary surface in a presence of the $U(1)$ external gauge field W_μ is written as [8]

$$i\gamma^\alpha e_\alpha{}^\mu(\nabla_\mu - iW_\mu)\psi = E\psi, \tag{2}$$

where $\nabla_\mu = \partial_\mu + \Omega_\mu$ with Ω_μ being the spin connection term, and e_α^μ being the zweibein. For three interesting geometries, the only nonzero components of Ω_μ and W_μ were found to be $W_\varphi = \nu$ and $\Omega_\varphi = i\omega\sigma^3$ where ν is the topological characteristics of the defect (the Frank index) and ω denotes the spin connection coefficients [8]. Notice that for massless fermions σ^3 serves as a conjugation matrix, and the energy eigenmodes in (2) are symmetric about $E = 0$ ($\sigma^3\psi_E = \psi_{-E}$). An elastic flow through a surface is given by a circular integral

$$\frac{1}{2\pi}\oint \vec{W}\,d\vec{r} = \nu.$$

Due to the symmetry group of the hexagonal lattice the possible values of the Frank index ν are multiplies of $1/6$.

The eigenfunctions in (1) are classified with respect to the eigenvalues of $J_z = j + 1/2$, $j = 0, \pm1, \pm2, \ldots$, and are to be taken in the form

$$\psi = \begin{pmatrix} u(r)e^{i\varphi j} \\ v(r)e^{i\varphi(j+1)} \end{pmatrix}. \tag{3}$$

The general analytical solution to (2) is known only for chosen geometries. One of them is the cone [7]. For the sphere and the hyperboloid, there were used some approximations. In particular, asymptotic solutions at small r (which allow us to study electronic states near the disclination line) were considered in [8]. We will study (2) numerically for all three geometries considering the case of the cone as a good test for our calculations.

3. Cone geometry

A cone can be constructed by cutting out a sector from a disk and then gluing the boundaries. In graphite lattice, a cutting of a 60° sector leads to a pentagonal defect which can be considered as apical disclination. Due to the symmetry of a graphite sheet only five types of cones can be created which are depend on the number n of removed sectors. The opening angle becomes directly connected to the Frank index of a disclination. The total disclinations of all these cones are multiplies of 60°, corresponding to the presence of a given number n of pentagons at the apices (evidently $\nu = n/6$). Notice that carbon nanocones with cone angles of 19°, 39°, 60°, 85°, and 113° have been observed in a carbon sample [14]. These angles might correspond to 300°, 240°, 180°, 120°, and 60° disclinations in graphite, respectively. Disks ($n = 0$) and one-open-end nanotube ($n = 6$) have also been observed in the same sample [14].

In the polar coordinates $(r, \varphi) \in R^2$ a cone can be regarded as an embedding

$$(r, \varphi) \to (ar\cos\varphi,\ ar\sin\varphi,\ cr),$$
$$0 < r < 1, \quad 0 \leqslant \varphi < 2\pi,$$

with a and c being the cone parameters. The opening angle of a cone, θ, is determined by $\sin(\theta/2) = a/\sqrt{a^2 + c^2}$. The Frank index of the apical disclination can be specified by $\nu = 1 - \sin(\theta/2)$. At $\nu = 0$ one gets a flat graphene sheet ($\theta = \pi$). For convenience, we introduce a parameter $\xi = 1 + c^2/a^2$, so that $\sin(\theta/2) = 1/\sqrt{\xi}$ and $1/\sqrt{\xi} = 1 - \nu$.

General representation for the zweibeins is found to be [8]

$$e^1{}_r = \sqrt{a^2 + c^2}\cos\varphi, \qquad e^1{}_\varphi = -ar\sin\varphi,$$
$$e^2{}_r = \sqrt{a^2 + c^2}\sin\varphi, \qquad e^2{}_\varphi = ar\cos\varphi.$$

The only nonzero components of the spin connection coefficients are

$$\omega_\varphi^{12} = -\omega_\varphi^{21} = 2\omega = 1 - 1/\sqrt{\xi}. \tag{4}$$

Making in (2) the substitution

$$\psi = \psi' r^\alpha, \quad \alpha = \sqrt{\xi}\,\omega,$$

one reduces the eigenvalue problem to

$$\partial_r u' - \frac{\sqrt{\xi}}{r}(j - \nu)u' = \widetilde{E}v',$$

$$-\partial_r v' - \frac{\sqrt{\xi}}{r}(j + 1 - \nu)v' = \widetilde{E}u', \tag{5}$$

where $\widetilde{E} = \sqrt{\xi}\,aE$. Eq. (5) allows for an exact solution. Namely, a general solution to (5) is found to be [8]

$$\begin{pmatrix} u' \\ v' \end{pmatrix} = Ar^{-\alpha}\begin{pmatrix} J_\eta(\widetilde{E}r) \\ \pm J_{\bar\eta}(\widetilde{E}r) \end{pmatrix} \tag{6}$$

with $\eta = \pm(\sqrt{\xi}\,(j - \nu + 1/2) - 1/2)$, and $\bar\eta = \pm(\sqrt{\xi}\,(j - \nu + 1/2) + 1/2)$. Despite the existence of the general solution to (5) we will present here also numerical calculations.

Some preliminary remarks should be done. We start the numerical calculations from the analytical asymptotic solutions found in [8]. The initial value of the parameter r is defined as $r = 10^{-4}$ in the case of the cone and sphere. It is worth noting that the choice of the boundary conditions does not influence the behavior of the calculated wave functions and only the starting point depends on it. A dimensionless substitution $x = Er$ in the case of the cone and sphere is used.

The normalized numerical solutions to (5) for different n are shown in Fig. 1. The parameters are chosen to be: $E = 0.01$, $a = 1$, and $c = 1$. We are also interested in the 'total' DOS on a patch $0 < r \leqslant \delta$ for small δ which can be written as (within a constant factor)

$$D(E, \delta) \sim \int_0^\delta \left(|u|^2 + |v|^2\right)\sqrt{g}\,dx^1. \tag{7}$$

The 'total' DOS near the Fermi energy for the cone is illustrated schematically in Fig. 2.

Here and below $\delta = 0.1$. Notice that in fact the choice of the value of δ does not influence the characteristic behavior of LDOS. One can see that the 'total' DOS has a cusp which drops to zero at the Fermi energy. It should be stressed that a specific behavior takes place only for $n = 3$ where a nonzero DOS near the Fermi energy is found.

4. Sphere (fullerene)

To describe a sphere we employ the polar projective coordinates $x^1 = r$, $x^2 = \varphi$; $0 \leqslant r < \infty$, $0 \leqslant \varphi <$

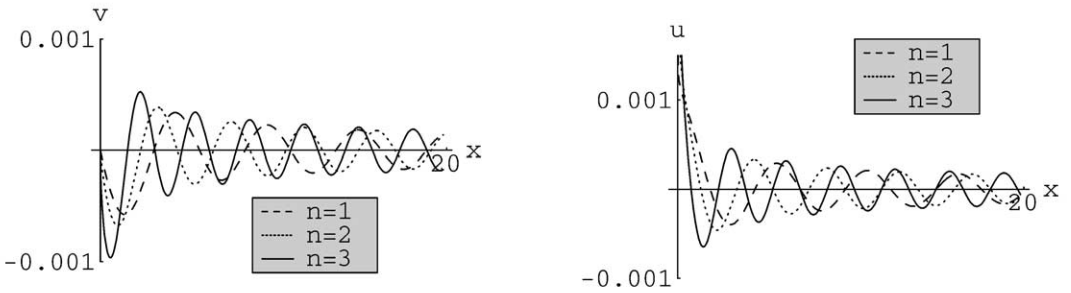

Fig. 1. The solutions $v(x)$, $u(x)$ for different n.

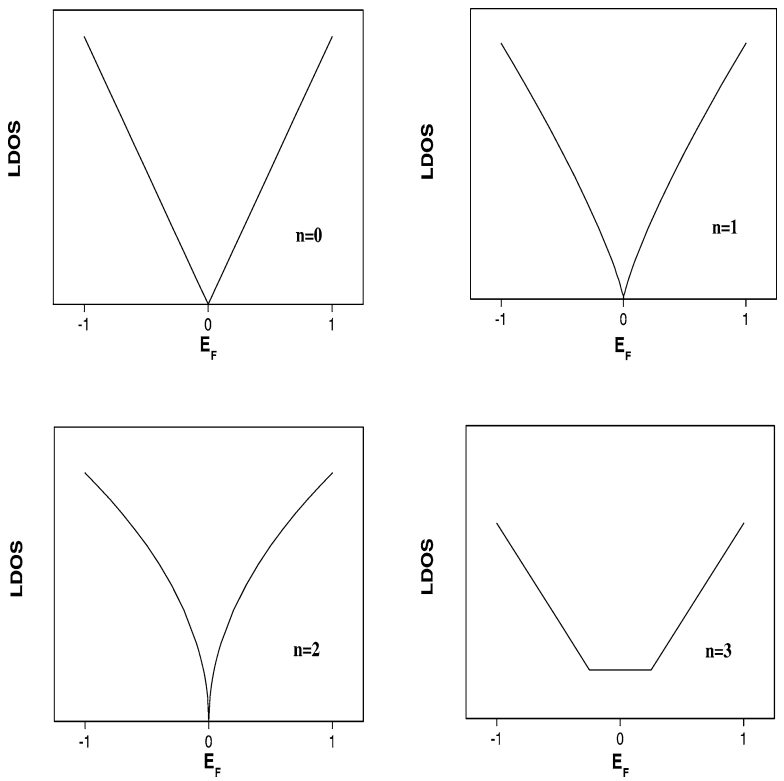

Fig. 2. Schematic densities of states near the Fermi energy in the case of cone.

2π with R being a radius of the sphere. A general representation for the zweibeins was found to be [8]

$$e^1{}_r = e^2{}_\varphi = 2R^2\cos\varphi/\left(R^2+r^2\right),$$

$$e^1{}_\varphi = -e^2{}_r = -2R^2\sin\varphi/\left(R^2+r^2\right),$$

which gives

$$\omega_\varphi^{12} = -\omega_\varphi^{21} = 2\omega = 2r^2/\left(R^2+r^2\right). \tag{8}$$

In this case, the spin connection term can be taken care of by redefining the wave function

$$\psi = \psi'\sqrt{R^2+r^2}, \tag{9}$$

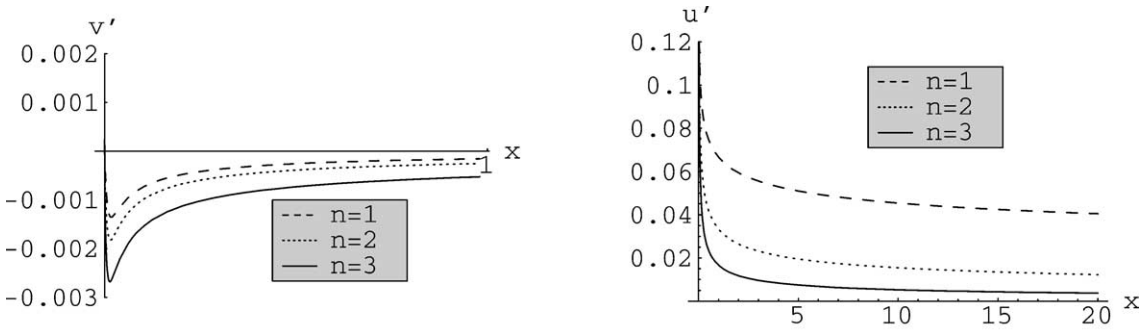

Fig. 3. The solutions $v'(x)$, $u'(x)$ for different n.

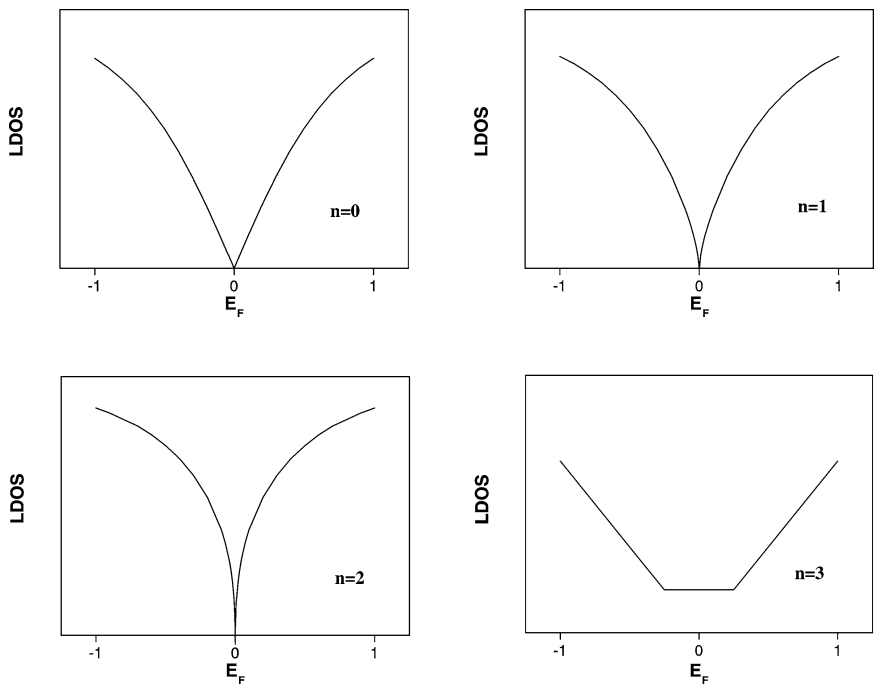

Fig. 4. Schematic densities of states near the Fermi energy in the case of sphere.

which reduces the eigenvalue problem (2) to

$$\partial_r u' - \frac{(j-\nu)}{r}u' = \widetilde{E}v',$$
$$-\partial_r v' - \frac{(j+1-\nu)}{r}v' = \widetilde{E}u', \tag{10}$$

where $\widetilde{E} = 2R^2E/(R^2+r^2)$.

The normalized numerical solutions to Eq. (10) are shown in Fig. 3. The chosen parameters are $E = 0.01$ and $R = 1$.

Notice that here we present the solutions for dotted values (v' and u') unlike the cone and hyperboloid geometries. In numerical calculations, the local DOS is taken as the maximum value of integrand in Eq. (7) depending on different values of energy (but taken near the Fermi energy). The results are shown schematically in Figs. 4, 5. Notice that the Fig. 5 describes also the dependence of the local DOS on a position of the maximum value of integrand (which actually characterizes the numerically calculated local-

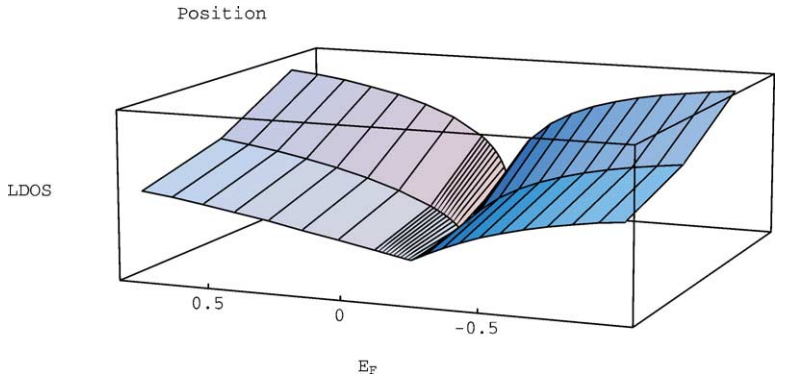

Fig. 5. 3d schematic plotting of the DOS near the Fermi energy for $n = 0, 1, 2$ (going from the front side to the back side).

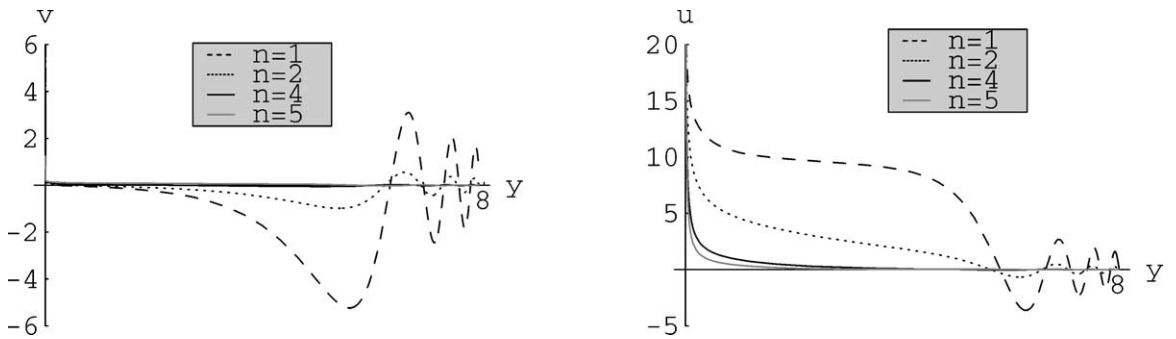

Fig. 6. Solutions $v(y)$, $u(y)$ for different n.

ization point of an electron). This could be of interest with relation to experiment.

As is seen, similarly to the case of the cone, the DOS has a cusp which drops to zero at the Fermi energy. However, for a sphere the behavior of curves differs from that in a cone. Again the case $n = 3$ becomes distinguished. It should be emphasized that in the fullerene molecule there are twelve 60° disclinations, so that the case $n = 1$ is actually realized.

5. Hyperboloid geometry

A single disclination on a finite graphite sheet is known to be buckled to screen its energy thus leading to curved hexagonal network [15]. One of the possible geometries is the hyperboloid. An upper half of a hyperboloid can be regarded as an embedding

$$(y, \varphi) \to (a \sinh y \cos\varphi, a \sinh y \sin\varphi, c \cosh y),$$
$$0 \leqslant y < \infty, \quad 0 \leqslant \varphi < 2\pi.$$

The zweibeins become [8]

$$e^1{}_y = \sqrt{g_{yy}} \cos\varphi, \qquad e^2{}_y = \sqrt{g_{yy}} \sin\varphi,$$
$$e^1{}_\varphi = -a \sinh y \sin\varphi, \qquad e^2{}_\varphi = a \sinh y \cos\varphi, \quad (11)$$

where $g_{yy} = a^2 \cosh^2 y + c^2 \sinh^2 y$. This gives for the nonzero spin connection coefficients

$$\omega^{12}_\varphi = -\omega^{21}_\varphi = \omega = \frac{1}{2}\left[1 - \frac{a \cosh y}{\sqrt{g_{yy}}}\right]. \quad (12)$$

The substitution

$$\psi' = \psi \sqrt{\sinh y}$$

reduces the eigenvalue problem (2) to

$$\partial_y u' - \sqrt{\coth^2 y + b^2}\, \tilde{j} u' = \widetilde{E} v',$$
$$-\partial_y v' - \sqrt{\coth^2 y + b^2}\, \tilde{j} v' = \widetilde{E} u', \quad (13)$$

where $\widetilde{E} = \sqrt{g_{yy}}\, E$, $b = c/a$, and $\tilde{j} = j - \nu + 1/2$.

The results of the numerical calculations are shown in Fig. 6 where the parameters are chosen to be $E =$

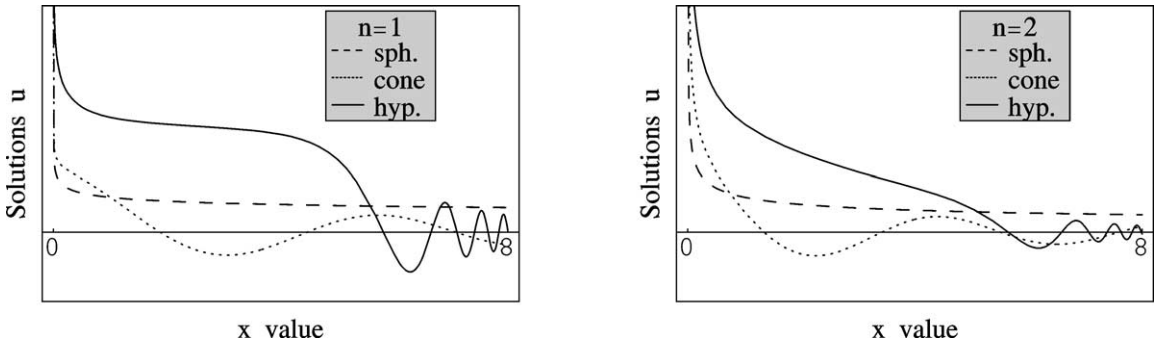

Fig. 7. The schematic pictures for $u(x)$ for three geometries in the case of $n = 1, 2$.

0.01, $a = 1$, and $c = 1$. Notice that the starting point in this case was chosen to be $y = 10^{-2}$.

The case of hyperboloid geometry differs from a cone and a sphere. Namely, there is a problem with the normalization of the solution for hyperboloid. Actually, the integrand is found to be constantly growing with increasing parameter y. Due to this problem (coming from the hyperboloid geometry itself) it is impossible to perform numerical calculations of the DOS.

6. Conclusion

To conclude, let us note that the solution for $u(u')$ is found to be of the decisive importance in the final results for all three geometries, which is consistent with the previous analytical results. To compare the behaviour of the solutions $u(u')$ for every kind of the geometries we show the combined pictures (see Fig. 7) for $n = 1, 2$. As it can be seen from the graphs the solutions for the sphere and hyperboloid have a similar behaviour near the disclination line at small $x(y)$, as it was predicted in the previous analytical calculations [8]. Notice that the choice of the parameters (R, c, a) does not influence the main characteristics of the calculated wave functions.

The numerical calculations confirm the finding that the pentagonal defects in graphite nanoparticles markedly modify the low-energy electronic structure. This is evident from both the exact form of wave functions and the local density of electron states. As is seen from the Fig. 5, in the case of sphere the local DOS increases with a distance from the disclination line for defects with $n = 0, 1, 2$. The low-energy total DOS has a characteristic cusp at the Fermi energy for any number of pentagons except $n = 3$ where the enhanced charge density at the Fermi energy is found. For nanocones this conclusion agrees with the results of [10] where the prominent peak, which appears just above the Fermi level, was established in a nanocone with three pentagons at the apex.

Acknowledgements

This work has been supported by the Science and Technology Department of Moscow region and the Russian Foundation for Basic Research under grant No. 01-02-97021 and by the Slovak Scientific Grant Agency, Grant No. 3197.

References

[1] D.L. Carroll, et al., Phys. Rev. Lett. 78 (1997) 2811.
[2] P. Kim, et al., Phys. Rev. Lett. 82 (1999) 1225.
[3] B. An, et al., Appl. Phys. Lett. 78 (2001) 3696.
[4] J. González, F. Guinea, M.A.H. Vozmediano, Phys. Rev. Lett. 69 (1992) 172;
J. González, F. Guinea, M.A.H. Vozmediano, Nucl. Phys. B 406 (1993) 771.
[5] V.A. Osipov, E.A. Kochetov, JETP Lett. 72 (2000) 199.
[6] C.L. Kane, E.J. Mele, Phys. Rev. Lett. 78 (1997) 1932.
[7] P.E. Lammert, V.H. Crespi, Phys. Rev. Lett. 85 (2000) 5190.
[8] V.A. Osipov, E.A. Kochetov, M. Pudlak, JETP 96 (2003) 140.
[9] K. Kobayashi, Phys. Rev. B 61 (2000) 8496.
[10] J.-C. Charlier, G.-M. Rignanese, Phys. Rev. Lett. 86 (2001) 5970.
[11] T. Yaguchi, T. Ando, J. Phys. Soc. Jpn. 71 (2002) 2224.
[12] D.P. DiVincenzo, E.J. Mele, Phys. Rev. B 29 (1984) 1685.
[13] E.A. Kochetov, V.A. Osipov, J. Phys. A: Math. Gen. 32 (1999) 1961.
[14] A. Krishnan, et al., Nature (London) 388 (1997) 451.
[15] D.R. Nelson, L. Peliti, J. Phys. (Paris) 48 (1987) 1085.